Evaluation of elastic stiffness in bolted timber joints for applying turn-of-nut method

Doppo Matsubara[1*] and Masaki Teranishi[2]

Abstract

The mechanical performance of bolt joints in wooden structures is known to vary significantly with the initial tightening force (axial force) of the bolts during the construction work. When a joining method that considers axial force is applied to a structure, the control of the axial force is important. This study attempts to evaluate the elastic stiffness of bolted timber joints during tightening for the purpose of applying the turn-of-nut tightening method, one of the methods for controlling axial force. Considering the elastic stiffness of joints during tightening as a series spring model using the spring constant of the bolt and the embedment spring constant of the washer, elastic stiffness is calculated using the washer embedment spring constant obtained through a washer embedment test. This result is compared with the elastic stiffness obtained through the tightening test using four species of timber. It was found that while the washer embedment spring constant varies greatly with timber species, the calculated values agreed well with the test results.

Keywords: Turn-of-nut, Bolted timber joints, Elastic stiffness, Tightening, Spring model

Introduction

The authors have developed a wood friction joint that utilizes the frictional resistance generated between members when bolts or lug screws are used to tighten timber members with other timber members or with steel plates, and a load-bearing wall in which these joints are embedded. The authors further demonstrated high seismic resistance in the wood friction joint through shaking table tests and other means [1, 2]. However, elucidation of the long-term stress relaxation behavior of timber and the establishment of a method for controlling the initial tightening force (hereinafter axial force) of the bolts, which manifest frictional resistance, are indispensable to the practical application of this wood friction joint. Regarding the long-term stress relaxation behavior of timber, it has been shown that, while temperature and humidity have influence when axial force in excess of the embedment yield of the timber is applied or when axial force is applied in the longitudinal direction of the timber, a relatively high axial force is maintained over a long period of time [3, 4]. Meanwhile, a torque-tightening method has been applied to control the axial force by using a general tool such as a torque wrench. It was demonstrated that the torque coefficient varies with the tightening rate [5, 6] and that the axial force of the lug screw reduces below the pull-out strength of the lug screw owing to the coefficient of friction of the threaded part [7, 8]. Although the torque method enables easy control of axial force, it greatly depends on the coefficient of friction of the threaded part of the bolts, etc., and the coefficient of friction of the seating surface. In addition, variations in axial force are unavoidable. Here, candidate methods for axial force control include the torque method as well as the turn-of-nut method. In the turn-of-nut method, seating is achieved using the relative tightening rotation angle between the bolt head and the nut as an indicator, after which the nut is rotated to the target angle to control axial force. However, with bolt joints made of ferrous material, the variation in the axial force in the elastic range using the turn-of-nut method is

*Correspondence: d.matsubara@fuk.kindai.ac.jp
[1] Kindai University, 11-6 Kayanomori, Iizuka, Fukuoka 820-8555, Japan
Full list of author information is available at the end of the article

as great as the variation using the torque method [9–11]. Conversely, when a material such as timber, which has a lower Young's modulus than ferrous materials, is used for the members to be joined, the gradient in the relationship between the rotation angle and axial force in the elastic region is considered less than that when a ferrous material is used. Accordingly, higher tightening accuracy can be expected than in the case in which the turn-of-nut method is applied to bolt joints made of ferrous materials. However, no studies have investigated the effectiveness of the turn-of-nut method applied to bolted timber joints as well as the elastic stiffness of joints during tightening, which is a key indicator for setting the rotation angle to achieve the target axial force.

Therefore, as the first step toward the application of the turn-of-nut method to bolted timber joints, this study considered a series spring model using the spring constant of bolts and the embedment spring constant of washers as a model for calculating the elastic stiffness of joints during tightening. It further calculated the elastic stiffness of joints during tightening by considering the washer embedment spring constant obtained through washer embedment testing. By comparing this calculation result with the elastic stiffness obtained from the findings of the wood bolt joint tightening tests in [12], the authors ascertained the degree to which the calculated values conform with the test results, and the findings are discussed.

Spring model

The model applies to bolted timber joints, as shown in Fig. 1. Considering the elastic stiffness K_j of a joint during tightening of the bolt as a series spring model using spring constant K_b for the bolt and embedment spring constant K_{ew} for the washer, the rotation angle ϕ during tightening can be calculated by the following equation:

$$\varphi = \frac{360}{P}\left(\frac{1}{K_b} + \frac{1}{K_{ew}}\right)F_b = \frac{360}{P}\frac{F_b}{K_j}. \tag{1}$$

Here, F_b is the axial force and P is the screw pitch. From (1), K_j can be calculated as

$$K_j = \frac{360}{P}\frac{F_b}{\varphi}, \tag{2}$$

or as

$$K_j = \frac{1}{\left(\frac{1}{K_b} + \frac{1}{K_{ew}}\right)}. \tag{3}$$

K_b can be calculated by the following equation [13] as a serial coupling of K_{th}, K_s, K_{cyl}, and K_{hd}, which are the spring constants for thread engagement (Fig. 1 ①), thread play (Fig. 1 ②), bolt cylinder (Fig. 1 ③), and bolt head (Fig. 1 ④):

$$\frac{1}{K_b} = \left(\frac{1}{K_{th}} + \frac{1}{K_s} + \frac{1}{K_{cyl}} + \frac{1}{K_{hd}}\right). \tag{4}$$

Here, K_{th}, K_s, K_{cyl}, and K_{hd} can be calculated by the following equations [13]:

$$K_{th} = \frac{A_s E_b}{L_{th}}, \tag{5}$$

$$K_s = \frac{A_s E_b}{L_s}, \tag{6}$$

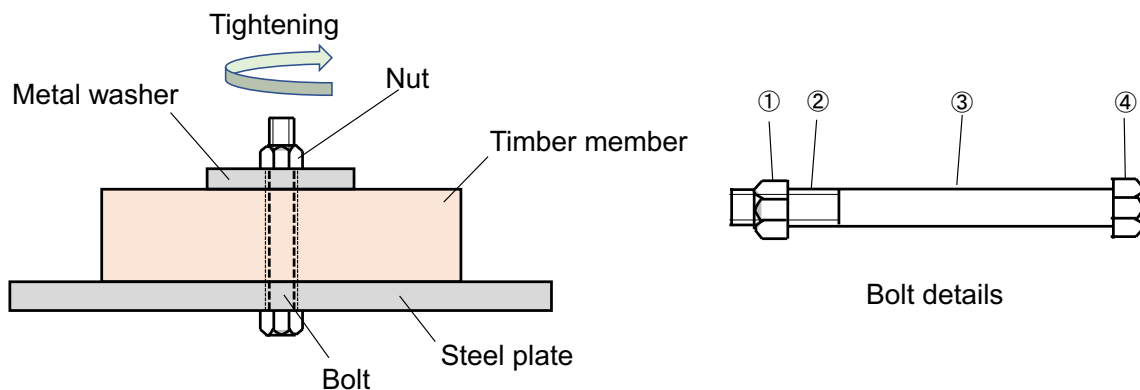$$K_{cyl} = \frac{A E_b}{L_{cyl}}, \tag{7}$$

Fig. 1 Bolted timber joints and bolt details

$$K_{hd} = \frac{AE_b}{L_{hd}},\tag{8}$$

where A_s is the effective cross-sectional area, whose value is obtained from JIS B1082 [14]; A is the cross-sectional area of the cylinder; and E_b is Young's modulus, which is set to 205,000 N/mm^2 here. L_s and L_{cyl} are the lengths of the thread play and the cylindrical part of the bolt. L_{th} and L_{hd} are the equivalent lengths of cylinders having the same axial stiffness as the thread engagement and the bolt head, and they can be calculated by the following equations in term of the bolt nominal diameter d [15]:

$$L_{th} = 0.85d,\tag{9}$$

$$L_{hd} = 0.55d.\tag{10}$$

## Materials and Methods
Tightening test [12]
An overview of the test setup is shown in Fig. 2. A tightening tester (NST-500 Nm, Japan Instrumentation System Co., Ltd.) was used for the testing. Timber test pieces were 90 mm in the tangential direction (T direction), 90 mm in the longitudinal direction (L direction), and 30 mm in the radial direction (R direction), with a ϕ13-mm bolt hole drilled in the center. Four types of timber were used: Japanese cedar (*Cryptomeria japonica*), southern Japanese hemlock (*Tsuga sieboldii*), hiba (*Thujopsis dolabrata*), and Japanese larch (*Larix kaempferi*).

For the test pieces, planks with dimensions of 90 mm in the T direction, 30 mm in the R direction, and 600 mm in the L direction were left in a chamber with a constant interior temperature of 20 °C and relative humidity (RH) of 50% for about 3 months. From these, test pieces free of knots were collected and used for testing. The tightening was performed to perpendicular to the grain. The density and moisture content of the test pieces are as shown in Table 1. Bolts were M12 hex bolts made of SWCH with chromate-treated surfaces, length 85 mm, screw pitch 1.75 mm, and thread length 30 mm. The metal washers were made of SPHC with width 40 mm, length 40 mm, and thickness 4.0 mm, with a ϕ14-mm bolt hole drilled in

Table 1 Basic properties of tightening test materials

Wood species		Density (kg/m^3)	Moisture content (%)
C. japonica	Ave	377	9.1
	S.D	32	0.5
T. sieboldii	Ave	507	8.5
	S.D	20	0.2
T. dolabrata	Ave	446	7.5
	S.D	4	0.1
L. kaempferi	Ave	669	9.2
	S.D	32	0.4

Ave average, *S.D* standard deviation

Fig. 2 Tightening test method (*L* longitudinal, *R* radial)
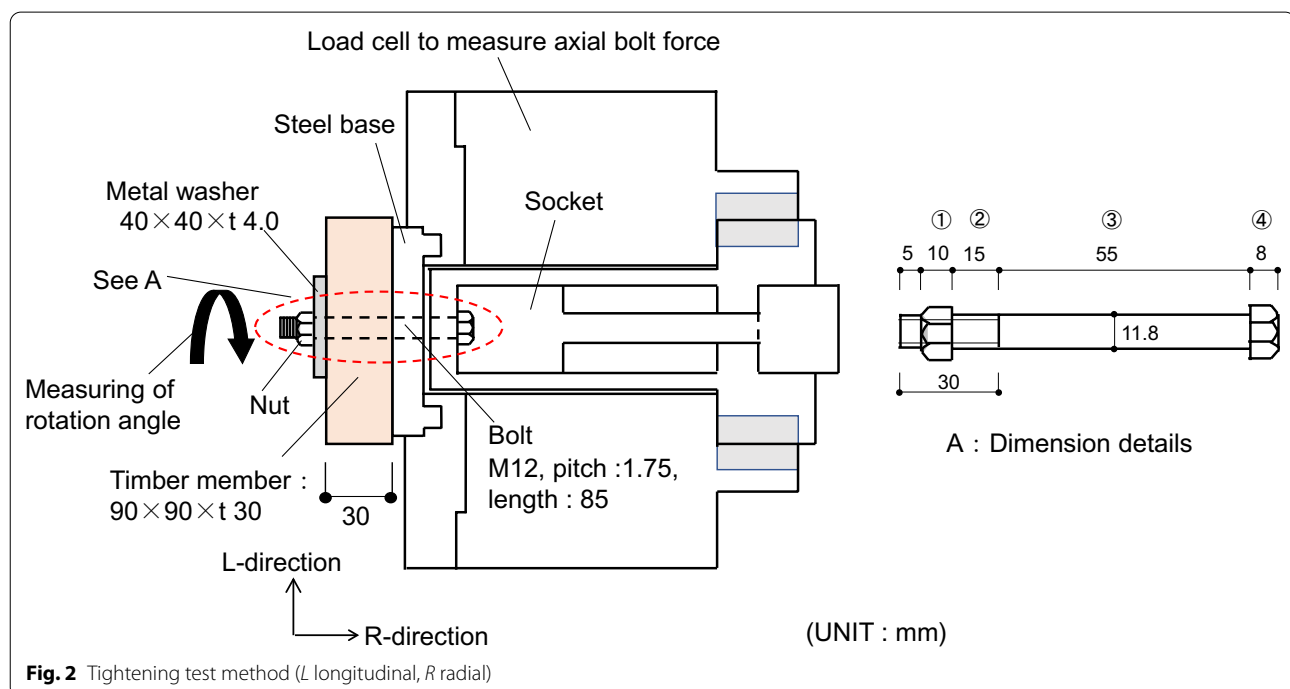
the center. In the testing, after the materials were placed on the testing apparatus, tightening was performed at a speed of 1.7 rpm on the nut side, axial force was measured with a load cell, and the nut rotation angle was measured. The nut was manually tightened, and the time when the axial force reached 10 N was set as the test start point. Based on the relationship between the obtained axial force and the rotation angle, the linear gradient of the elastic region was calculated using the least squares method, and elastic stiffness $K_{j\text{-}exp}$ of the joint was calculated by Eq. (2). For each wood species, 12 specimens were used.

Embedment test of metal washers

To obtain the washer embedment spring constant K_{ew}, a washer embedment test was conducted using the surplus plank material left over from the tightening test. In the testing, monotonic loading was performed perpendicular to the grain as shown in Fig. 3, using a universal testing machine (AG-100kNIS, Shimadzu Corporation). The testing speed was 3 mm/min. Specifications of the timber test pieces and the washers were identical to those in the tightening test. The density and moisture content of the test pieces are as shown in Table 2. The crosshead stroke of the universal testing machine was used as the amount of displacement, measured as the average of the readings from the displacement meters attached on the test table at two locations. Based on the relationship between the obtained load and displacement, the linear gradient of the elastic region was calculated using the least squares

Table 2 Basic properties of embedment test materials

| Wood species		Density (kg/m³)	Moisture content (%)
C. japonica	Ave	392	8.8
	S.D	22	0.5
T. sieboldii	Ave	504	7.8
	S.D	9	0.4
T. dolabrata	Ave	446	7.5
	S.D	6	0.1
L. kaempferi	Ave	670	9.2
	S.D	25	0.6

Ave average, S.D standard deviation

method and was used as K_{ew}. For each wood species, 12 specimens were used.

Results and Discussion

Axial bolt force–rotation angle and load–displacement relationships

Figure 4 shows the representative relationship between the axial force and the rotation angle obtained by the tightening test. Figure 5 shows the representative relationship between the load and displacement obtained by the washer embedment test. As shown in Fig. 4, at the initial stage, the axial force increased little as the rotation angle increased, and the slip behavior was exhibited. The axial force increased almost linearly through

Fig. 3 Schematic of the apparatus for the embedment test (*L* longitudinal, *R* radial)

Fig. 4 Relationship between axial bolt force and rotation angle obtained by tightening test

Fig. 5 Relationship between load and displacement obtained by embedment test
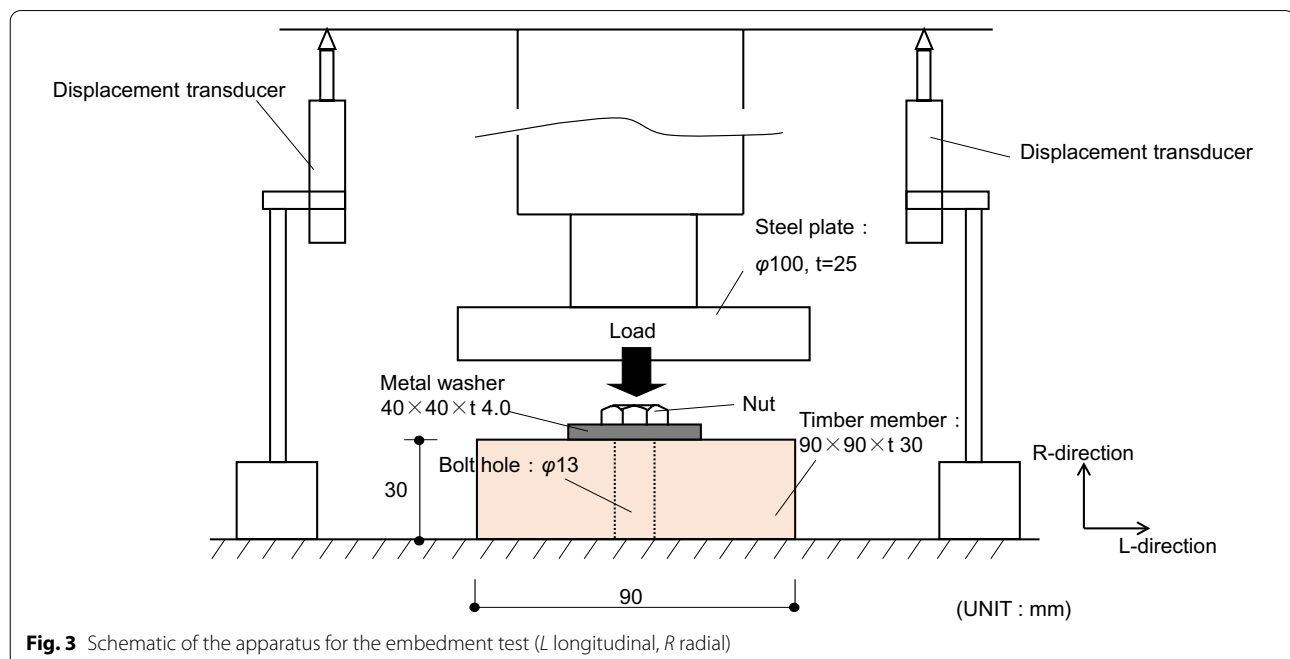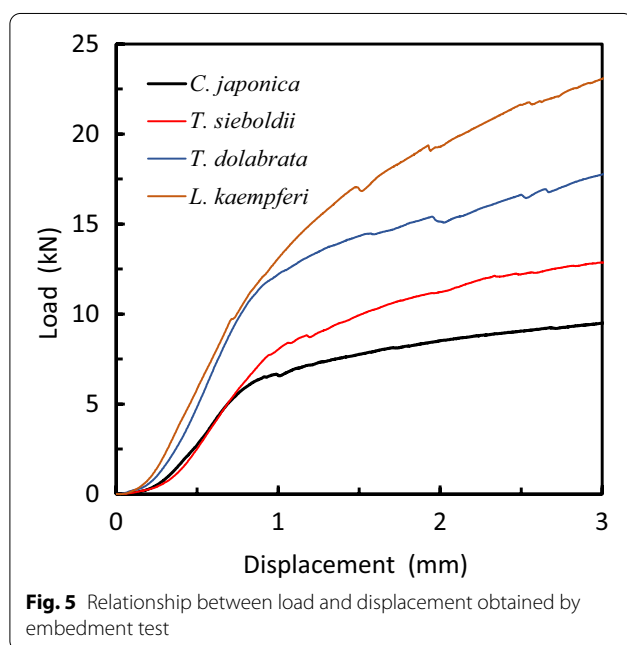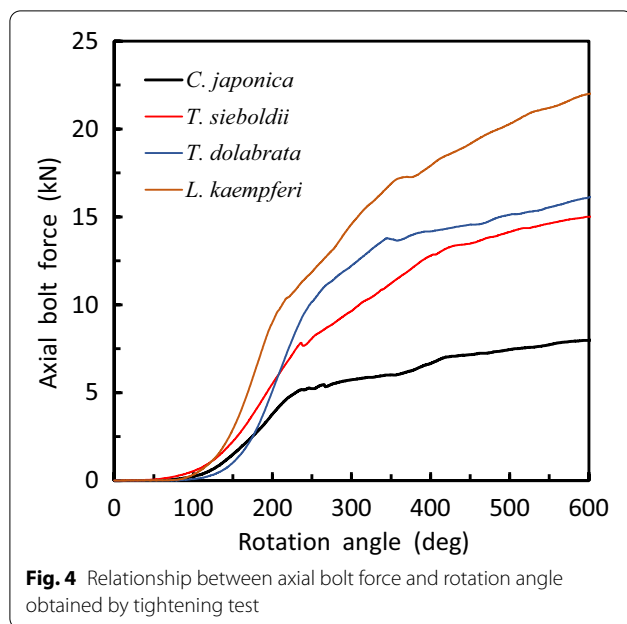
the so-called snag point [16], after which it exhibited a tendency to increase non-linearly. These behaviors were nearly identical to the relationship between washer embedment load and displacement shown in Fig. 5. Here, the yield stress of the bolt used in the test was not investigated; however, on the assumption that it corresponds to bolt tensile strength rank 4.8, the bolt's yield axial force was approximately 27 kN. In Fig. 4, if the axial force point at which the nearly linear portion changes to a non-linear

portion is defined as the yield axial force, then the yield axial force of each test piece is clearly less than the bolt's yield axial force of 27 kN. Accordingly, the yield axial force of each test piece can be recognized as nearly identical to the yield load of each test piece in Fig. 5, and can be inferred to be manifested by the washer embedment.

Calculation of K_j in bolted timber joints using K_{ew}

Table 3 shows $K_{j\text{-exp}}$ obtained through the tightening test, K_{ew} obtained through the washer embedment test, and $K_{j\text{-cal}}$ calculated from Eq. (3). Here, $K_{j\text{-exp}}$ and K_{ew} were derived using the least squares method, with intervals of 2–4 kN for *C. japonica* and *T. sieboldii* and 4–6 kN for *T. dolabrata* and *L. kaempferi* assumed as the linear gradients in the elastic region. The results indicate that $K_{j\text{-cal}}$ was 1.2 times $K_{j\text{-exp}}$ for *C. japonica*, but the values were generally in agreement for other wood species. Figure 6 shows the relationship between $K_{j\text{-exp}}$, $K_{j\text{-cal}}$, and density for the test pieces of each wood species. For *C. japonica* and *L. kaempferi*, both $K_{j\text{-exp}}$ and $K_{j\text{-cal}}$ tended to increase as density increased. For *L. kaempferi*, the distributions of $K_{j\text{-exp}}$ and $K_{j\text{-cal}}$ nearly overlap. In case of $K_{j\text{-cal}}$ for *C. japonica*, the test piece group with a density of over 400 kg/m^3 exhibited a high value. From this test piece group, it can be understood that the difference between $K_{j\text{-cal}}$ and $K_{j\text{-exp}}$ in Table 3 increased. For *T. dolabrata*, no clear tendency was seen in the relationship between density and $K_{j\text{-exp}}$ or $K_{j\text{-cal}}$; however, the distributions of $K_{j\text{-exp}}$ and $K_{j\text{-cal}}$ can be seen to generally overlap. Conversely, for *T. sieboldii*, $K_{j\text{-exp}}$ was clearly lower in five test pieces than in the remaining test pieces; however, the distributions of $K_{j\text{-exp}}$ and $K_{j\text{-cal}}$ in the remaining test pieces generally overlapped.

These results indicate that elastic stiffness K_j during the tightening of bolted timber joints can be calculated with high accuracy using the embedment spring constant K_{ew} of the washer and the spring constant K_b of the bolt. In addition, assuming that the turn-of-nut method is applied to bolted timber joints, it can be understood

Table 3 Comparative of $K_{j\text{-exp}}$ and $K_{j\text{-cal}}$

Wood species		$K_{j\text{-exp}}$ (kN/mm)	$K_{j\text{-cal}}$ (kN/mm)	K_{ew} (kN/mm)
C. japonica	Ave	11.5	14.0	14.9
	S.D	2.5	3.5	3.5
T. sieboldii	Ave	12.1	12.0	12.6
	S.D	3.4	1.9	1.9
T. dolabrata	Ave	18.3	19.6	21.4
	S.D	4.4	1.5	1.5
L. kaempferi	Ave	19.4	18.3	19.9
	S.D	6.4	3.6	3.6

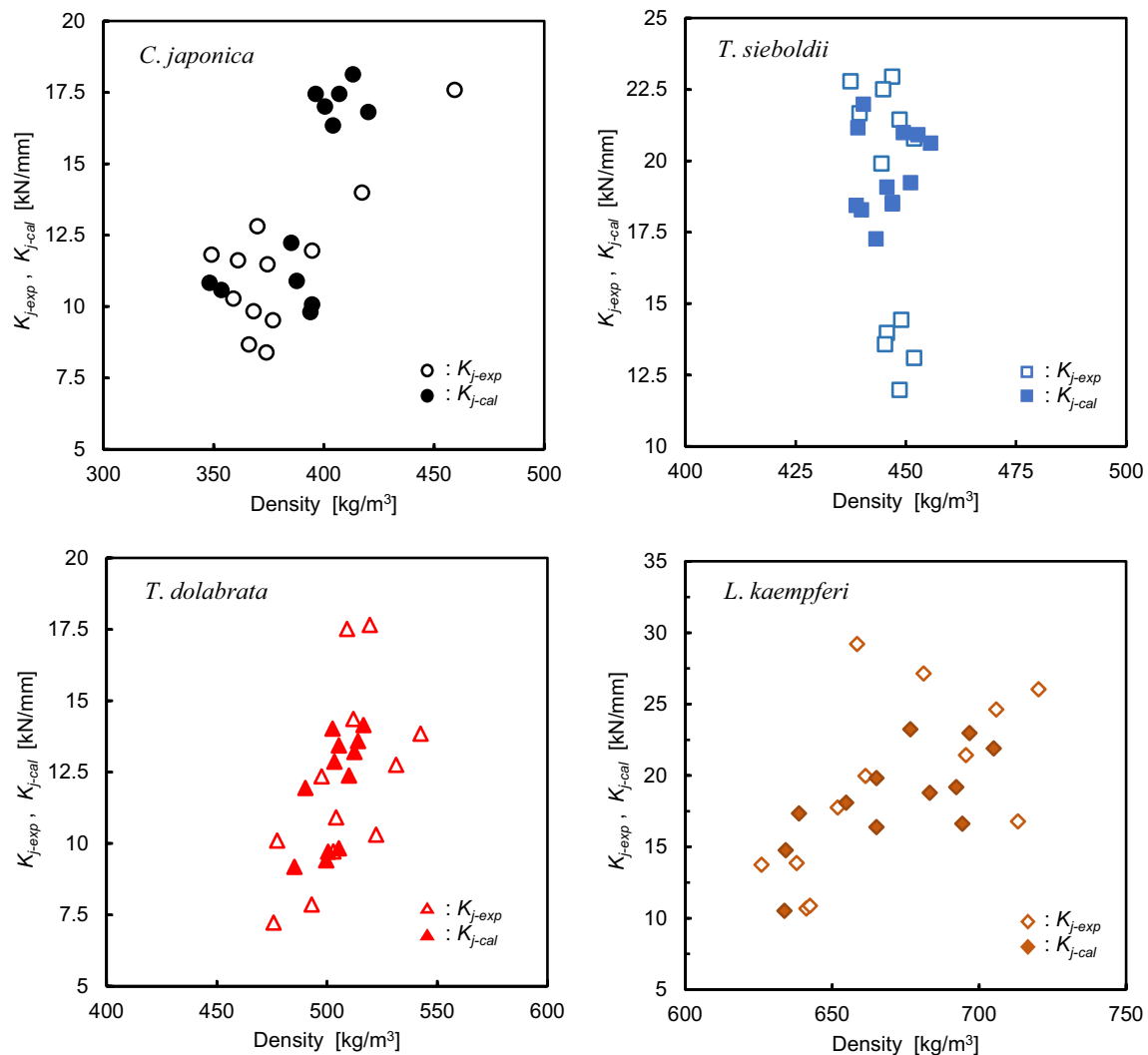*Ave* average, S.D standard deviation

Fig. 6 Relationship between K_{j-exp}, K_{j-cal}, and density

from Eq. (3) that lowering K_b or K_{ew} will decrease K_j. However, Fig. 6 shows that variation in K_{ew}, while differing in degree according to wood species, is unavoidable. Furthermore, it can be predicted that K_j will change depending on timber thickness. We hope to further investigate on how this variation in K_{ew} and effect of timber thickness affects tightening accuracy in application of the turn-of-nut method.

Conclusions

The elastic stiffness of joints during tightening, an important index for setting the rotation angle to obtain target axial force for bolted timber joints, was considered and calculated from a series spring model using

the spring constant of bolts and the embedment spring constant of washers. This was compared with the elastic stiffness obtained from the tightening test. The findings of the study are as follows:

(1) The relationship between the axial force and the rotation angle obtained from the tightening test conducted for four wood species was similar to the relationship between load and displacement obtained from the washer embedment test conducted for the four wood species. Furthermore, the relationships initially show slipping properties, after which the axial force and load increased nearly linearly. However, from the point of yield onward, a non-linear relationship was displayed. In addition,

the yield axial force was manifested by the embedment of the washer.

(2) The results calculated using the series spring model was able to capture the results of the tightening test, and the calculation can be performed with high accuracy.

At the same time, the embedment spring constant of the washers exhibited considerable variation. The effect of this variation on tightening accuracy under the turn-of-nut method remains a topic for further study.

Declarations

Ethics approval and consent to participate
Not applicable.

Consent for publication
We agree to allow our manuscript being published.

Competing interests
The authors declare that they have no competing interests.

Author details
[1]Kindai University, 11-6 Kayanomori, Iizuka, Fukuoka 820-8555, Japan. [2]Niigata University, 8050, Ikarashi 2-no-cho, Nishi-ku, Niigata 950-2181, Japan.

References
1. Ishikawa K, Wakashima Y, Fujioka R, Shimizu H, Matsubara D, Kitamori A (2021) Contributions of plywood shear walls and plasterboards on seismic response reduction of timber structures using wood friction-based dampers. AIJ J Technol Des 27(65):166–171 (**in Japanese**)
2. Wakashima Y, Ishikawa K, Shimizu H, Kitamori A, Matsubara D, Tesfamariam S (2021) Dynamic and long-term performance of wood friction connectors for timber shear walls. Eng Str. https://doi.org/10.1016/j.engstruct.2021.112351
3. Wakashima Y, Kitamori A, Shimizu H, Ishikawa K, Matsubara D (2019) Relaxation of wood under temperature and humidity changes. Summaries of Technical Papers of Annual Meeting, Architectural Institute of Japan, Structures III pp 1–2
4. Wakashima Y, Shimizu H, Kitamori A, Matsubara D, Ishikawa K, Fujisawa Y (2019) Stress relaxation behavior of wood in the plastic region under indoor conditions. J Wood Sci 65:1–9
5. Matsubara D, Nakano T, Shimada M, Funada R, Hattori N (2015) Effect of tightening velocity on the torque coefficient of timber jointing with bolts. Mokuzai Gakkaishi 61(1):33–39
6. Matsubara D, Wakashima Y, Fujisawa Y, Shimizu H, Kitamori A, Ishikawa K (2018) Effects of tightening speed on torque coefficient in lag screw timber joints with steel side plates. J Wood Sci 64:112–118
7. Matsubara D, Wakashima Y, Fujisawa Y, Shimizu H, Kitamori A, Ishikawa K (2017) Relationship between clamp force and pull-out strength in lag screw timber joints. J Wood Sci 63:625–634
8. Matsubara D, Wakashima Y, Fujisawa Y, Shimizu H, Kitamori A, Ishikawa K (2019) A novel method for estimating ultimate clamp force in lag screw timber joints with steel side plates. Trans Mater Res Soc Jpn 44:109–113
9. Fukuoka T, Takaki T (2004) Evaluations of the tightening process of bolted joint with elastic angle control method. In: Proceedings of pressure vessels and piping conference, California, 25–29 July 2004
10. JIS B1083–2008 (2008) General rules for tightening of threaded fasteners. Japanese Standard Association, Tokyo, p 807 (**in Japanese**)
11. Brown W (2011) Utilizing the turn-of-nut method to stop gasketed bolted joint leakage. In: Proceedings of pressure vessels and piping conference, Maryland, 17–21 July 2011
12. Matsubara D, Shimada M, Nishikawa Y, Nakano T, Hattori N (2014) Relationship between tightening torque and clamp force on bolted joints of timber. Mokuzai Kogyo 69:19–23 (**in Japanese**)
13. Fukuoka T, Kageyama K, Kusafuka H, Hirao M (2018) New bolt tightening method with high accuracy utilizing real-time measurement of nut factor. Mar Eng 53(4):124–129
14. JIS B1082–1987 (2008) Stress area and bearing area for threaded fasteners. Japanese Standard Association, Tokyo, p 795 (**in Japanese**)
15. Fukuoka T (1992) Analysis of the tightening process of a bolted with a tensioner. Estimation by means of spring elements. Trans Jpn Soc Mech Eng Series A 58(549):760–764 (**in Japanese**)
16. JIS B1083–2008 (2008) General rules for tightening of threaded fasteners. Japanese Standard Association, Tokyo, p 810 (**in Japanese**)